Vol. 14(1): 48-59, January 2026 DOI: https://doi.org/10.23960/jsl.v14i1.1256

Jurnal Sylva Lestari

P-ISSN: 2339-0913
E-ISSN: 2549-5747

Journal homepage: https://sylvalestari.fp.unila.ac.id

Full Length Research Article

Cooling Rates of Mahogany (*Swietenia macrophylla* King.) and Yemane (*Gmelina arborea* Roxb.) Determined by Infrared Thermography and Its Relationship to Density

Prince Ranier Cacaos Rana*, Oliver Segundo Marasigan

Forest Products Research and Development Institute (FPRDI), Department of Science and Technology (DOST), College, Laguna, Philippines
* Corresponding author. E-mail address: pcrana1@up.edu.ph

ARTICLE HISTORY:

Received: 29 August 2025
Peer review completed: 1 November 2025
Received in revised form: 24 November 2025
Accepted: 3 December 2025

KEYWORDS:

Gmelina arborea
Infrared thermography
Nondestructive testing
Rate of cooling
Swietenia macrophylla

ABSTRACT

Determining wood density is essential for assessing its mechanical properties and industrial suitability, yet traditional methods are destructive and impractical for standing trees or finished products. This study investigates the application of infrared thermography (IRT) as a rapid, nondestructive method for estimating wood density from cooling behavior. Mahogany (*Swietenia macrophylla* King.) and yemane (*Gmelina arborea* Roxb.), two economically important plantation species in the Philippines, were examined under controlled heating and natural cooling conditions. Twelve samples with varying densities at 60°C were analyzed, and their cooling curves were modeled using the first-term transient plane-wall solution. A strong inverse correlation was found between density and cooling rate constant (k_{app}), with coefficients of determination (R^2) values of 0.90 for mahogany and 0.97 for yemane, confirming that denser samples cooled more slowly. Additionally, a 21% difference in cooling rates between mahogany and yemane at similar densities suggests that species-specific characteristics may influence heat loss. These results demonstrate the potential of IRT as a rapid, nondestructive tool for estimating wood density, with applications in timber grading, quality assessment, and forest resource monitoring; accordingly, this approach could be adapted for rapid on-site density estimation in timber grading and monitoring.

1. Introduction

Mahogany (*Swietenia macrophylla* King.) and yemane (*Gmelina arborea* Roxb.) are among the most widely cultivated industrial tree plantation species (ITPS) in the Philippines. These species are valued for their rapid growth, favorable wood properties, and adaptability to plantation management, making them key sources of timber for the domestic market. They are extensively used in construction, furniture manufacturing, paneling, and veneer production due to their workability and versatility (Abarquez et al. 2015; Alipon et al. 2019; Cossid et al. 2025; Gilbero et al. 2019; Marasigan et al. 2025). In 2022, the DENR–FMB (2023) reported that mahogany contributed 65,870.62 m³ and yemane 26,599.08 m³ to the country's plantation timber production. A key determinant of the suitability of these woods for such uses is their density, a physical property strongly correlated with strength, durability, dimensional stability, and machinability. Density is also a critical parameter for classifying timber, predicting mechanical performance, and

ensuring quality control in industrial applications (Xin et al. 2022). In conventional practice, density is determined using ASTM D2395 test methods for wood and wood-based materials (ASTM International 2022).

Traditionally, destructive methods such as oven-drying and weighing yield exact wood density but are impractical for standing trees or finished products. Nondestructive testing (NDT) is therefore preferred to estimate density via indirect measurements correlated with it (Henriques et al. 2025). NDT approaches investigated include organoleptic, acoustic, and quasi-non-destructive techniques. Organoleptic methods are qualitative and evaluator-dependent (Josifovski et al. 2023). Acoustic stress wave and ultrasonic techniques relate wave velocity to timber density but can be limited by internal cracks that distort measured velocities (Duong and Kanninen 2024; Íñiguez-González et al. 2015; Martiansyah et al. 2022; Tiitta et al. 2020). Additionally, quasi-non-destructive tests, such as the pilodyn, screw withdrawal, and resistograph drilling, show strong correlations between density and penetration depth or withdrawal resistance (Bobadilla-Maldonado et al. 2025; Henriques et al. 2025). In parallel with these techniques, Infrared thermography (IRT) has also advanced in recent years, with applications in building inspection and wood evaluation (Fox et al. 2019; Pitarma et al. 2019; Vössing and Niederleithinger 2018).

IRT is a promising NDT method that maps surface temperature based on emitted infrared radiation, allowing detection of thermal patterns without physical contact (Azzi et al. 2025; Qu et al. 2020). In active IRT, a controlled heat source is applied to the specimen, and the surface temperature is monitored during the cooling phase. Because wood's thermal conductivity (k_t), specific heat capacity (c_p), and diffusivity (α) are influenced by density and moisture content, cooling behavior therefore carries information about these properties (Hung Anh and Pásztory 2021; Jang and Kang 2022). Denser wood generally stores more heat and thus cools more slowly than lighter wood of the same initial temperature, assuming similar specific heat capacity (Maeda et al. 2021). Conversely, low-density wood tends to release heat more quickly, resulting in a steeper temperature drop. This principle suggests that the cooling rate of a heated wood sample could serve as an indirect indicator of its density.

Indeed, previous studies have found that surface temperature decay parameters measured by IRT correlate with wood density and moisture content (Antikainen et al. 2015; Borghese et al. 2024; López et al. 2018). López et al. (2018) demonstrated that the variation in surface temperature during cooling is statistically related to density, enabling quantitative density estimates via thermographic data. They reported that by 10 minutes into the cooling phase, the linear correlation between temperature drop and density reached an $R^2 > 0.95$. Similarly, Antikainen et al. (2015) successfully used active IR heating and imaging to estimate the moisture content of birch veneer, noting that thermal decay rates were sensitive to differences in density and moisture. These works collectively suggest that IRT, which has been used qualitatively in the past (e.g., to identify wet or decayed zones in structures), can be developed into a quantitative tool for evaluating wood properties (Borghese et al. 2024; Xin et al. 2021).

However, the applicability of active IRT for tropical plantation-grown hardwoods remains underexplored, especially for high-value species such as mahogany and yemane. Although these species are widely cultivated and utilized in the Philippines (Alipon et al. 2019; Cossid et al. 2025; Gilbero et al. 2019), few studies have investigated active IRT for estimating density or other mechanical properties in these species. Recent IRT work linking thermal decay to density/mechanics focuses on non-Philippine taxa and contexts (Borghese et al. 2024; López et al.

2018; Xin et al. 2021, 2022). Consequently, the applicability of tropical plantation-grown timbers remains uncertain, leaving a gap in understanding despite their high economic importance to the country. Addressing this knowledge gap is essential for determining the potential of IRT in tropical hardwood quality assessment.

To address this gap, the present study applies the IRT cooling rate approach to mahogany and yemane samples, aiming to quantify the relationship between their thermal decay parameters and measured densities and to evaluate the feasibility of IRT as a rapid, nondestructive method for density estimation, providing a scientific basis for its integration into wood quality assessment and potential adoption in industrial and field applications where speed, accuracy, and preservation of the material are essential.

2. Materials and Methods

2.1. Sample Preparation

Mahogany and yemane samples were collected from Candelaria and Tiaong, Quezon Province, Philippines, respectively. The trees were approximately 15 to 30 years old. Following the method of López et al. (2018), six samples per species, representing varying densities, were cut to 15 cm × 20 cm × 2 cm and sanded with 800-grit paper for uniform surface conditions (**Table 1**).

Table 1. Density of mahogany and yemane at 60°C

Species	Sample	Density (kg/m³)
Mahogany	1	680.96
	2	640.27
	3	563.20
	4	530.71
	5	519.26
	6	512.24
	Average	574.44
Yemane	1	512.22
	2	502.46
	3	482.58
	4	464.90
	5	435.19
	6	406.65
	Average	467.33

The 2-cm thickness was oriented in the radial direction (pith-to-bark), with the 15 cm × 20 cm face tangential, and this orientation was kept identical for all specimens. Each sample was placed in a Fisher Scientific Isotemp 650G oven and heated to 60°C until thermal equilibrium was achieved. A K-type thermocouple (TECPEL DTM-318) attached to a representative specimen monitored the heating process, with equilibrium defined as a stable reading within ± 0.5°C for at least 10 minutes. Care was taken to position the samples uniformly inside the oven and to avoid direct contact with the oven walls to minimize temperature gradients (**Fig. 1**). Immediately upon removal from the oven, each specimen was quickly weighed using a SHIMADZU UX8200S digital balance to determine its mass. Volume was calculated from the measured dimensions, and the corresponding density at 60°C (kg/m³) using Equation 1.

$$\rho_{60} = \frac{M_{60}}{V_{60}} \quad (1)$$

where ρ_{60}, M_{60}, and V_{60} is the density (kg/m³), mass (kg), and volume (m³) of the sample at 60°C, respectively.

Fig. 1. Setup for heating wood samples using a Fisher Scientific Isotemp 650G oven.

After weighing, the surface temperature of each sample was measured using a Fluke iSee™ TC01A mobile thermal camera, set at a fixed emissivity of 0.90, as used by López et al. (2018). The camera, mounted perpendicular to the sample on a tripod, captured thermal images at consistent framing to allow accurate cooling-curve analysis. Ambient temperature and relative humidity were recorded using a Lascar EasyLog EL-WiFi-TH sensor placed near the sample. Transfer and imaging were performed with minimal air disturbance and in the shortest possible time to reduce uncontrolled cooling before measurement.

Each specimen was subjected to a single heating-cooling cycle to avoid surface alteration that could influence emissivity or thermal response in subsequent trials. This procedure followed the approach of López et al. (2018), who also applied a single heating-cooling cycle per sample when modeling temperature decay using infrared thermography. Although replicate thermal measurements were not performed on the same specimen, care was taken to maintain identical heating conditions and environmental parameters across all samples. Exact replication at identical densities was not feasible due to natural variability inherent to the wood; however, specimens were selected within a relatively narrow density range for each species to capture representative thermal behavior. This limitation is acknowledged as it may introduce minor variability in the cooling parameters obtained.

Following the initial temperature capture, each specimen was allowed to cool naturally under stable laboratory conditions (Temp 25°C; RH 60%), free from forced air or direct sunlight. Surface temperatures were recorded at predetermined intervals of 1, 2, 5, 10, 20, 30, 40, 50, and 60 minutes. Each thermal image was analyzed to determine the average temperature within the pre-defined region of interest. The difference between the temperature of the wood surface and the ambient air

(ΔT_t) was calculated for every time point. To determine the appropriate heat transfer model, the Biot number is expressed by Equation 2.

$$Bi = \frac{hL_c}{k_t} \quad (2)$$

Biot number was evaluated because it quantifies the ratio of internal conduction resistance to external convection resistance: small Bi ($\approx \leq 0.1$) indicates an almost uniform internal temperature suitable for a lumped model, whereas larger Bi signals non-negligible internal gradients that require transient conduction solutions (Bergman et al. 2017; Lienhard and Lienhard 2024). The plane-wall characteristic length $L_c = t/2 = 0.01$ m (thickness $t = 0.02$ m, radial direction) was used, together with species-specific transverse conductivities for mahogany and yemane at ~12% MC (k_t = 0.170,0.164 W/m^{-1}·K^{-1}) from guarded hot-plate measurements (Mundin and Acda 2025) and a still-air free-convection envelope $h \approx 2 – 25$ W/m^{-2}·K^{-1} for gases (Bergman et al. 2017; Çengel and Ghajar 2020). These inputs yielded $Bi \approx 0.12 – 1.47$ (mahogany) and 0.12 – 1.52 (yemane), exceeding the small Bi criterion for a strictly lumped model (Lienhard and Lienhard 2024). Late-time cooling was therefore modeled using the first-term transient plane-wall solution, fit to Equation 3.

$$ln\left(\frac{\Delta T_t}{\Delta T_0}\right) = -k_{app}t \quad (3)$$

where ΔT_t is the temperature difference at time t (°C), ΔT_0 is the initial difference at $t = 0$ (°C), and k_{app} is the apparent first-term decay constant (min^{-1}); for a plane wall, $k_{app} = \lambda_1^2 \alpha / L_c^2$ with $\alpha = k_t/(\rho_{60} c_p)$, and $\lambda_1 \tan \lambda_1 = Bi$ (Lienhard and Lienhard 2024).

2.2. *Statistical Analysis*

A linear regression was performed on the plot of ln $(\Delta T_t/\Delta T_0)$ versus t to determine the k_{app} for each specimen. The coefficient of determination (R^2) was used to assess how well the cooling process followed Equation 3. The resulting k_{app} values served as the primary thermal parameter for evaluating the relationship between cooling behavior and density at test. The calculated k_{app} values were then compared with the corresponding densities at 60°C for all 12 specimens to evaluate the relationship between density and cooling behavior. This analysis aimed to determine whether denser wood samples exhibited slower cooling rates, indicative of higher thermal inertia. The resulting correlation provides a basis for assessing the potential of infrared thermography as a nondestructive method for estimating wood density.

3. Results and Discussion

Infrared thermography revealed consistent cooling behavior across all wood samples, showing a clear relationship between density and thermal response (**Fig. 2**). Denser specimens consistently cooled more slowly than less dense ones. This trend was observed both within and between species. Mahogany, with a higher density range (512–681 kg/m³), retained heat for longer than yemane (407–512 kg/m³). Within each species, samples with higher density exhibited more gradual declines in surface temperature, indicating slower thermal dissipation.

This behavior is primarily governed by the material's volumetric heat capacity, which depends on its density and specific heat capacity. Because the specific heat capacity of wood remains relatively constant across species (typically around 1.3 $kJ \cdot kg^{-1} \cdot K^{-1}$), the variation in heat storage and release is mainly controlled by density (Glass and Zelinka 2021). As a result, denser samples possess higher thermal mass and store more energy, leading to slower temperature changes during cooling.

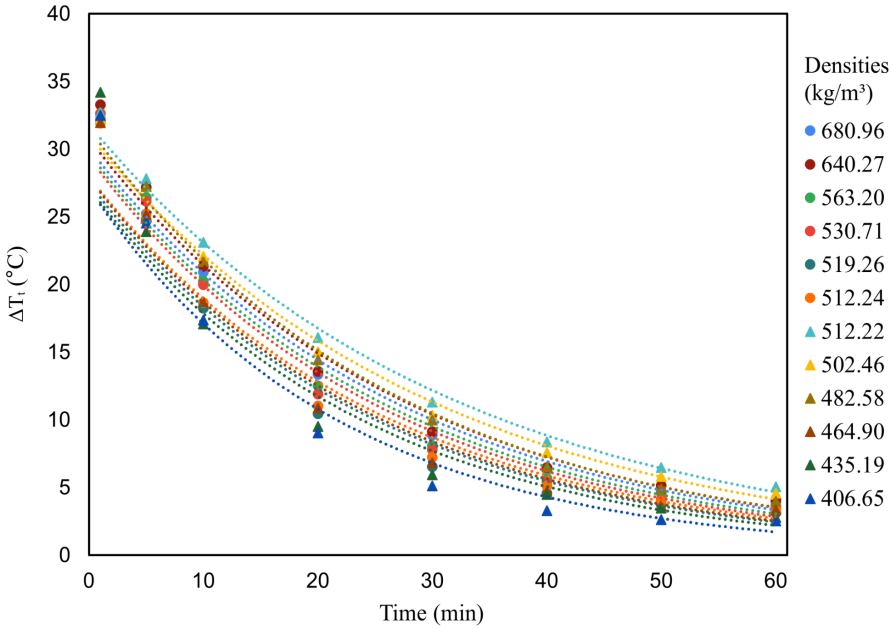

Fig. 2. Temperature variation of mahogany (circles) and yemane (triangles) wood samples during cooling. Curves show surface temperature difference (ΔT_t) relative to room temperature. Denser samples cooled more slowly due to higher thermal mass.

Empirical studies reinforce this explanation. Beall (1968) found no significant variation in specific heat capacity among wood species, identifying density as the dominant factor in thermal storage capacity. Similar findings were reported by Goss (1992) and TenWolde et al. (1988), who observed proportional increases in thermal mass with rising density across various wood types. In addition, wood's low thermal diffusivity (approximately 10^{-7} m^2/s) limits the rate of heat propagation, particularly in denser specimens, further slowing cooling.

As shown in **Fig. 2**, this principle is evident in the cooling curves, where mahogany samples consistently exhibit a more gradual temperature decline than yemane samples. To analyze the cooling behavior more precisely, the data for each sample were fitted to Equation 3. Plotting the surface temperature difference on a semi-logarithmic scale ($ln\,(\Delta T_t/\Delta T_0)$ vs. time) produced nearly linear trends for all specimens (**Fig. 3**), confirming that the cooling process followed a first-order exponential decay. These fits allowed the extraction of k_{app} for each sample, with high coefficients of determination (R^2 values ranging from 0.94 to 0.99), indicating excellent model agreement. **Table 2** summarizes the density, fitted equations, and corresponding R^2 values for each sample.

The relationship between the decay constant and density is shown in **Fig. 4,** where an inverse correlation is evident for both species. As density increases, the fitted cooling constant k_{app} decreases, indicating slower heat dissipation. Under the first-term transient plane-wall model with

$Bi > 0.1$, $k_{app} = \lambda_1^2 \alpha / L_c^2$, and $\alpha = k_t/(\rho_{60} c_p)$; with c_p varying weakly near room temperature and transverse k_t of similar order for these hardwoods, the increase in ρ_{60} lowers α and therefore reduces k_{app} (Bergman et al. 2017; Lienhard and Lienhard 2024; Mundin and Acda 2025). Small offsets between species at comparable density likely reflect anatomical effects on k_t and interfacial heat transfer. Overall, the monotonic decline of k_{app} with density is consistent with first-mode transient conduction rather than a lumped-capacitance response.

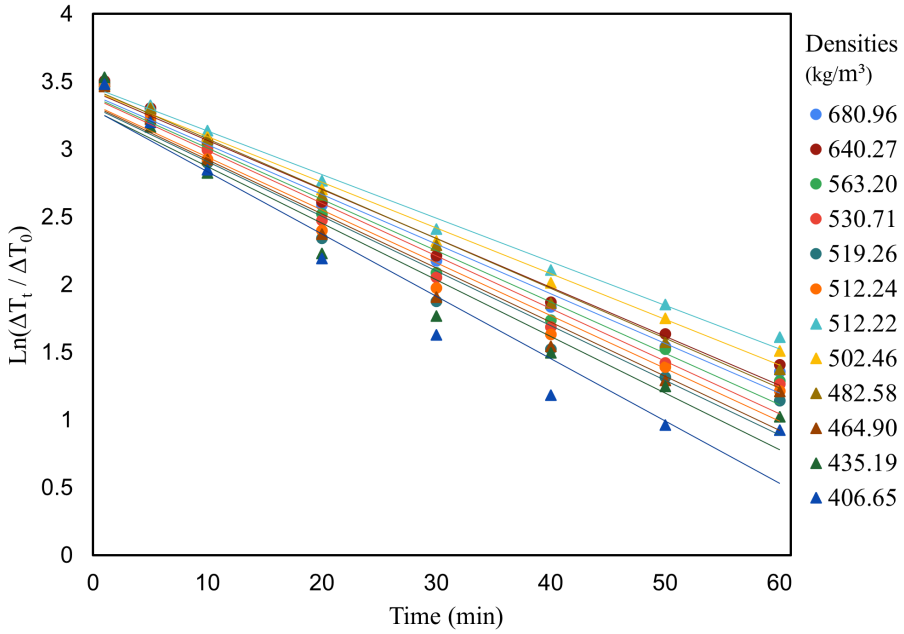

Fig. 3. Semi-logarithmic plots of $ln\ (\Delta T_t/\Delta T_0)$ versus time for mahogany (circles) and yemane (triangles). Near-linear trends indicate exponential cooling behavior, with shallower slopes in denser samples reflecting lower cooling rates.

Table 2. Summary of sample density, fitted exponential cooling equations, and R^2 values for mahogany and yemane

Species	Density (kg/m³)	$T_{initial}$ (°C)	T_{final} (°C)	ΔT	Function $\Delta T_t = \Delta T_0 e^{-k_{app}t}$	R^2 (exponential)	R^2 (linear)
Mahogany	680.96	59.90	29.40	30.50	$30.051e^{-0.0368x}$	0.99	0.98
	640.27	60.00	29.40	30.60	$30.759e^{-0.0362x}$	0.98	0.98
	563.20	59.55	28.70	30.85	$29.698e^{-0.0379x}$	0.98	0.98
	530.71	60.60	28.70	31.90	$29.392e^{-0.0389x}$	0.98	0.97
	519.26	59.00	27.90	31.10	$27.493e^{-0.0404x}$	0.97	0.96
	512.24	60.20	28.50	31.70	$27.971e^{-0.039x}$	0.98	0.97
Yemane	512.22	60.60	31.00	29.60	$31.791e^{-0.0322x}$	0.99	0.99
	502.46	59.70	30.50	29.20	$31.003e^{-0.0338x}$	0.99	0.99
	482.58	59.15	29.30	29.85	$31.492e^{-0.0368x}$	0.99	0.99
	464.90	59.90	28.40	31.50	$27.876e^{-0.04x}$	0.98	0.96
	435.19	61.80	28.10	33.70	$27.159e^{-0.0419x}$	0.95	0.95
	406.65	59.70	27.70	32.00	$27.101e^{-0.0461x}$	0.97	0.94

These results also corroborate previous IRT studies. Xin et al. (2021) reported a strong negative correlation ($R^2 \approx 0.977$) between cooling behavior and wood density in historical timber

using active IRT. Similarly, López et al. (2018) demonstrated statistically significant correlations between wood density and cooling rate across multiple species, with R^2 values exceeding 0.95. These studies, along with the gathered results, support the use of cooling rate constants as robust, nondestructive indicators of wood density under controlled moisture and thermal conditions.

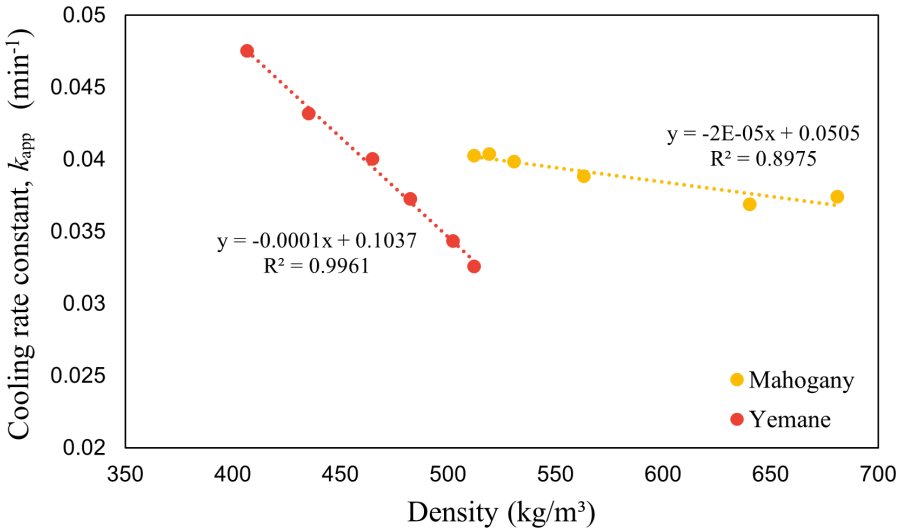

Fig. 4. Relationship between cooling constant (k_{app}) and wood density. The inverse trend indicates slower heat dissipation in denser samples, resulting from higher thermal mass and reduced thermal diffusivity.

Although density was the primary factor governing the cooling constant k_{app}, subtle interspecies differences in k_{app} were observed. At the sole near-overlap in density (~512 kg/m³), the linear fits for the two species differ by 21%, reported as a relative percent difference based on the two predicted k_{app} values at the same density. Given the limited overlap and small sample size, this percentage is a single-point, illustrative estimate and not a general species effect. Differences in anatomical structure may contribute: Mahogany is diffuse-porous with relatively uniform vessel distribution, whereas yemane is semi-ring-porous and often has larger earlywood vessels (Escobin et al. 2015); such features can influence internal heat-transfer pathways and surface exchange, potentially yielding slightly higher k_{app} at similar density for yemane.

Furthermore, species-specific differences in extractive content (such as oils, resins, or other deposits) can affect density and thermal conductivity by altering the cell wall structure or filling lumens. While these microstructural and compositional factors likely contribute to the observed intra-density variation in cooling rates, their influence was secondary. The dominant trend remained clear: increased density corresponded to reduced cooling rates, as reflected in lower k_{app} values across both species.

4. Conclusions

Infrared thermography effectively captured the cooling behavior of mahogany and yemane, revealing distinct thermal responses among specimens. Wood samples with higher density consistently exhibited slower cooling rates, reflecting greater thermal inertia. Notably, even at similar densities, mahogany and yemane exhibited differences in cooling rates, likely due to anatomical variations that influence heat transfer pathways. The gradual loss of heat in denser

specimens can be attributed to their higher volumetric heat capacity and reduced thermal diffusivity, both of which contribute to slower temperature decay. Estimated Biot numbers for the tested geometry and still-air conditions exceeded the small-*Bi* threshold, indicating non-uniform internal temperatures; consequently, cooling was interpreted using the first-term transient plane-wall model rather than a lumped-capacitance model. These results confirm that cooling behavior, as measured by IRT, is strongly linked to density and modulated by wood structure, supporting its potential as a nondestructive tool for density estimation and wood quality assessment. To translate this approach to field practice, future work should quantify moisture-content effects and validate portable, in situ measurements on standing trees to establish operational limits.

Acknowledgments

The authors gratefully acknowledge the Department of Science and Technology (DOST) and the DOST–Philippine Council for Industry, Energy, and Emerging Technology Research and Development (PCIEERD) for providing financial support. They also extend thanks to the Physics and Mechanics Section of DOST-FPRDI, especially Mr. Pigar, Mr. Fuentes, Mr. Elleva, and Mr. Dimapilis, for their help in preparing the samples. Appreciation is given to Ms. K Delmo, Ms. K Samonte, and Ms. R Hayag for their assistance with data acquisition and the management of surface temperature measurements. Special recognition goes to Dr. RJ Cabangon and Mr. FC Pitargue for their invaluable support. The authors further acknowledge the efforts of the DOST-FPRDI Collection team, led by Mr. Roxas, for their contribution in gathering wood samples, as well as the Promotion and Communication Section for their help with language editing.

Author Contributions

P.R.C.R.: Conceptualization, Methodology, Software, Validation, Formal Analysis, Investigation, Resources, Data Curation, Writing – Original Draft Preparation, Writing – Review and Editing, Visualization, Supervision, Project Administration, Funding Acquisition; O.S.M.: Conceptualization, Methodology, Software, Validation, Formal Analysis, Investigation, Resources, Data Curation, Writing – Original Draft Preparation, Writing – Review and Editing, Visualization, Supervision, Project Administration, Funding Acquisition.

Conflict of Interest

The authors declare no conflict of interest.

Declaration of Generative AI and AI-Assisted Technologies in the Manuscript Preparation

Not applicable.

References

Abarquez, A., Bush, D., Ata, J., Tolentino, E. L., and Gilbero, D. 2015. Early Growth and Genetic Variation of Mahogany (*Swietenia macrophylla*) in Progeny Tests Planted in Northern Mindanao, Philippines. *Journal of Tropical Forest Science* 27(3): 314–324.

Alipon, M. A., Bondad, E. O., Alcachupas, P. L., and Cortiguerra, E. C. 2019. Properties and Utilization of Young-Age Yemane (*Gmelina arborea* Roxb.) for Lumber Production. *Philippine Journal of Science* 148(1): 139–148.

Antikainen, T., Rohumaa, A., Bulota, M., Kotilahti, T., and Hughes, M. 2015. Estimating Birch Veneer (*Betula pendula* Roth) Moisture Content Using Infrared Technology. *European Journal of Wood and Wood Products* 73(5): 617–625. DOI: 10.1007/s00107-015-0944-7

ASTM International. 2022. *Standard Test Methods for Density and Specific Gravity (Relative Density) of Wood and Wood-Based Materials*. American Society for Testing and Materials.

Azzi, Z., Al Sayegh, H., Metwally, O., and Eissa, M. 2025. Review of Nondestructive Testing (NDT) Techniques for Timber Structures. *Infrastructures* 10(2): 28. DOI: 10.3390/infrastructures10020028

Beall, F. 1968. *Specific Heat of Wood*. Research Note FPL–0184. Department of Agriculture, Forest Service, Forest Products Laboratory. Madison, WI. U.S.

Bobadilla-Maldonado, I., Martinez-Lopez, R., Matini-Behzad, H., and Hillig, E. 2025. Physical and Mechanical Aging of Wood-Plastic Composites: Nondestructive Methods for Quality Control. *Wood Science and Technology* 27: e2025. DOI: 10.22320/s0718221x/2025.18

Bergman, T. L., Lavine, A. S., Incropera, F. P., and DeWitt, D. P. 2017. *Fundamentals of Heat and Mass Transfer*. 8th ed. John Wiley and Sons, Hoboken.

Borghese, V., Santoro, L., Santini, S. and Sesana, R. 2024. Correlation between Thermal and Density Properties of Chestnuts: Preliminary Results of Experimental Nondestructive Testing. *Archives of Civil and Mechanical Engineering* 24(3): 157. DOI: 10.1007/s43452-024-00969-8

Çengel, Y. A., and Ghajar, A. J. 2020. *Heat and Mass Transfer: Fundamentals and Applications*. 6th ed. McGraw-Hill Education, New York.

Cossid, R. N., Torralba, J. M. A., Clemente, J. H. M., Villaflor, C. J. G., Jandug, C. M. B., and Casilac Jr, C. S. 2025. Bending Strengths of Large-leaf Mahogany (*Swietenia macrophylla* King) and Mangium (*Acacia mangium* Willd) Commercial Lumbers in Northeastern Mindanao, Philippines. *Jurnal Sylva Lestari* 13(1): 317–331. DOI: 10.23960/jsl.v13i1.1072

Department of Environment and Natural Resources - Forest Management Bureau (DENR–FMB). 2023. 2022 *Report: Production of Major Forest Products*. Quezon City, Philippines.

Duong, D. V., and Kanninen, M. 2024. Variation of Stress Wave Velocity, Wood Density, and Static Bending Strength of 22-Year-Old Planted *Tectona grandis* Trees in Northwest Vietnam. *Journal of Tropical Forest Science* 36(4): 416–423. DOI: 10.26525/jtfs2024.36.4.416

Escobin, R. P., America, W. M., Pitargue, F. C., and Conda, J. M. 2015. *Revised Wood Identification Handbook for Philippine Timber, Volume 1*. Department of Science and Technology, Forest Products Research and Development Institute.

Fox, B., McWade, P., and Cashell, K. 2019. Infrared Thermography for Qualitative Assessment of Historic Timber Structures. *Proceedings of the Institution of Civil Engineers – Engineering History and Heritage* 172(4): 168–177. DOI: 10.1680/jenhh.18.00023

Gilbero, D. M., Abasolo, W. P., Matsuo-Ueda, M., Kamiya, N., Nakada, R., and Tanabe, J. 2019. Surface Growth Stress and Wood Properties of 8-Year-Old Planted Big-Leaf Mahogany (*Swietenia macrophylla* King) from Different Landrace Provenances and Trial Sites in the Philippines. *Journal of Wood Science* 65(1): 35. DOI: 10.1186/s10086-019-1814-4

Glass, S. V., and Zelinka, S. L. 2021. Moisture Relations and Physical Properties of Wood. In *Wood Handbook: Wood as An Engineering Material* (Chap. 4). Forest Service, Forest Products Laboratory. Madison, U.S.

Goss, W. P., and Miller, R. G. 1992. Thermal Properties of Wood and Wood Products. *Proceedings of the Thermal Performance of the Exterior Envelopes of Buildings Conference.* Oak Ridge National Laboratory, U.S. pp. 193–203.

Henriques, D. F., Şen, A. U., and Gomes, M. d. G. 2025. Assessing the Density of Wood in Heritage Buildings' Elements Through Expedited Semi-Destructive Techniques. *Applied Sciences* 15(13): 7552. DOI: 10.3390/app15137552

Hung Anh, L. D., and Pásztory, Z. 2021. An Overview of Factors Influencing Thermal Conductivity of Building Insulation Materials. *Journal of Building Engineering* 43(3): 102604. DOI: 10.1016/j.jobe.2021.102604

Íñiguez-González, G., Montón, J., Arriaga, F., and Segués, E. 2015. In-Situ Assessment of Structural Timber Density using Nondestructive and Semi-Destructive Testing. *BioResources* 10(2): 2256–2265.

Jang, E., and Kang, C. W. 2022. The Relationship between Bulk Density and Thermal Conductivity in Various Korean Woods. *Wood Research* 67(2): 178–186. DOI: 10.37763/wr.1336-4561/67.2.178186

Josifovski, A., Todorović, N., Milošević, J., Veizović, M., Pantelić, F., Aškrabić, M., Vasov, M., and Rajčić, A. 2023. An Approach to In Situ Evaluation of Timber Structures Based on Equalization of Nondestructive and Mechanical Test Parameters. *Buildings* 13(6): 1405. DOI: 10.3390/buildings13061405

Lienhard, J. H., V, and Lienhard, J. H., IV. 2024. *A Heat Transfer Textbook*. 6th ed. Cambridge, Phlogiston Press, MA.

López, G., Basterra, L. A., and Acuña, L. 2018. Infrared Thermography for Wood Density Estimation. *Infrared Physics and Technology* 89: 242–246. DOI: 10.1016/j.infrared.2018.01.015

Maeda, K., Tsunetsugu, Y., Miyamoto, K., and Shibusawa, T. 2021. Thermal Properties of Wood Measured by the Hot-Disk Method. *Journal of Wood Science* 67(1): 50. DOI: 10.1186/s10086-021-01951-1

Marasigan, O. S., Daguinod, S. A., and Villareal, J. F. 2025. Physico-Mechanical Properties of Two Native Tree Species in the Philippines and Their Potential as Alternatives to Exotic Industrial Tree Plantation Species. *Environment and Natural Resources Journal* 23(4): 343–356. DOI: 10.32526/ennrj/23/20250038

Martiansyah, I., Zulkarnaen, R. N., Hariri, M. R., Hutabarat, P. W. K., and Wardani, F. F. 2022. Tree Health Monitoring of Risky Trees in the Hotel Open Space: A Case Study in Rancamaya, Bogor. *Jurnal Sylva Lestari* 10(2): 180–201. DOI: 10.23960/jsl.v10i2.570

Mundin, M. A. M., and Acda, M. N. 2025. Thermal Conductivity of Plantation Wood Species and Selected Tropical Hardwoods from the Philippines. *BioResources* 20(3): 6877–6886. DOI: 10.15376/biores.20.3.6877-6886

Pitarma, R., Marques, G., and Ferreira, B. R. 2019. Infrared Thermography in Building Inspection: An Overview of Recent Advancements. *Applied System Innovation* 2(4): 44. DOI: 10.3390/asi2040044

Qu, Z., Jiang, P., and Zhang, W. 2020. Development and Application of Infrared Thermography Nondestructive Testing Techniques. *Sensors* 20(14): 3851. DOI: 10.3390/s20143851

TenWolde, A., McNatt, J. D., and Krahn, L. 1988. *Thermal Properties of Wood and Wood-Based Materials*. Department of Agriculture, Forest Service, Forest Products Laboratory. Madison, WI, U.S.

Tiitta, M., Tiitta, V., Gaal, M., Heikkinen, J., Lappalainen, R., and Tomppo, L. 2020. Air-Coupled Ultrasound Detection of Natural Defects in Wood Using Ferroelectret and Piezoelectric Sensors. *Wood Science and Technology* 54: 1051–1064. DOI: 10.1007/s00226-020-01189-y

Vössing, J., and Niederleithinger, E. 2018. Advancements in Nondestructive Testing of Wood Using Ultrasound and Infrared Thermography. *Proceedings of the 18th International Conference on NDT of Wood*. Berlin, Germany.

Xin, Z., Guan, C., Zhang, H., Yu, Y., Liu, F., Zhou, L., and Shen, Y. 2021. Assessing the Density and Mechanical Properties of Ancient Timber Members Based on the Active Infrared Thermography. *Construction and Building Materials* 304(6): 124614. DOI: 10.1016/j.conbuildmat.2021.124614

Xin, Z., Ke, D., Zhang, H., Yu, Y., and Liu, F. 2022. Nondestructive Evaluation of Ancient Timber Members' Density and Mechanical Properties Using Machine Learning and Thermography. *Construction and Building Materials* 341(6): 127855. DOI: 10.1016/j.conbuildmat.2022.127855